

# We are IntechOpen, the world's leading publisher of Open Access books Built by scientists, for scientists

6,900

Open access books available

186,000

International authors and editors

200M

Downloads

Our authors are among the

154

Countries delivered to

TOP 1%

most cited scientists

12.2%

Contributors from top 500 universities



WEB OF SCIENCE™

Selection of our books indexed in the Book Citation Index  
in Web of Science™ Core Collection (BKCI)

Interested in publishing with us?  
Contact [book.department@intechopen.com](mailto:book.department@intechopen.com)

Numbers displayed above are based on latest data collected.  
For more information visit [www.intechopen.com](http://www.intechopen.com)



# An Approach Based on Synthetic Organic Chemistry Toward Elucidation of Highly Efficient Energy Transfer Ability of Peridinin in Photosynthesis

Takayuki Kajikawa and Shigeo Katsumura  
*Kwansei Gakuin University*  
*Japan*

## 1. Introduction

Photosynthesis has driven the development of life which is powered by the efficient capture and conversion of sunlight. Carotenoids are naturally occurring pigments that absorb sunlight in the spectral region in which the sun irradiates maximally. These molecules transfer the absorbed energy to chlorophylls and the primary photochemical events of photosynthesis are initiated. More than a half of photosynthesis is performed in the ocean, although the oceanic photosynthesis is relatively less studied. Marine carotenoid, peridinin, has been known as the main light-harvesting pigment in photosynthesis in the sea and forms the unique water soluble peridinin-chlorophyll a (Chl a)-protein (PCP) complex. The crystal structure of the main form of the PCP trimer from *Amphidinium carterae* was determined by X-ray crystallography as shown in Fig. 1 (A) (Hoffman et al., 1996). Each of the polypeptides binds eight peridinin molecules and two Chl a molecules, and the allene function of peridinin exists in the center of the PCP. In this complex, a so-called antenna pigment, peridinin exhibits exceptionally high (> 95%) energy transfer efficiencies to Chl a (Song et al., 1976; Mimuro et al., 1993). This energy transfer efficiency is thought to be related to the unique structure of peridinin, which possesses allene and ylidenebutenolide functions and the unusual C37 carbon skeleton referred to as a 'nor-carotenoid' (Fig. 1 (B)) (Stain et al., 1971). There are, however, no studies on the relationship between the structural features of peridinin and its super ability for the energy transfer in the PCP complex.

In order to clear this efficient energy transfer mechanism, there are many and hot discussions in spectroscopic fields. In particular, the presence of an intramolecular charge transfer (ICT) excited state of peridinin has been proposed. It has been anticipated that the highly efficient energy transfer is caused through this key energy level, and a detailed discussion on this is described in the later chapters. This particular excited state is thought to be related to the intricate structure of peridinin. However, the precise nature of the ICT excited state and its role in light-harvesting have not yet been entirely clear, and there are no studies on the relation between the structural features of peridinin and its super ability for the energy transfer in the PCP complex. This is because the synthesis of various kinds of desired peridinin derivatives are not easy. Then, we started the research work to clear the

subjects of why peridinin possesses a unique allene group, a ylidenebutneolide ring and an irregular C37 skeleton, and how these functions play a role in the exceptionally high energy transfer and in the special excited state, ICT state.

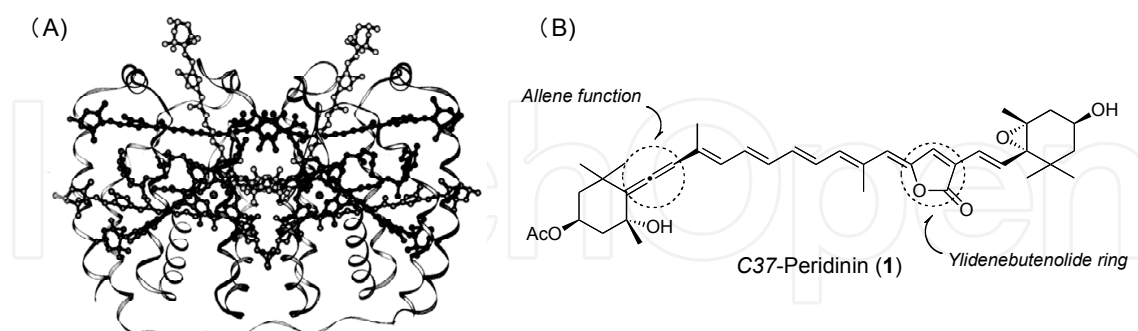


Fig. 1. (A) Crystal structure of PCP complex and (B) the structure of peridinin

## 2. Syntheses and stereochemical characteristics of peridinin derivatives

### 2.1 Design of peridinin derivatives and synthetic strategy

We have focused on the subjects of why peridinin possesses a unique allene group, a ylidenebutenolide ring and the irregular C37 carbon not to be usual C40 skeleton, how these functional groups play a role in the exceptionally high energy transfer, and how they affect the ICT state. In order to solve these questions, we designed and began to synthesize allene-modified, ylidenebutenolide-modified and conjugated chain-modified derivatives of peridinin (Fig. 2). For example, in order to understand the exact roles of the allene group, we designed following three peridinin derivatives. Acetylene derivative **2** possesses an epoxy-acetylene, olefin derivative **3** has an epoxy-olefin, and diolefin derivative **4** has a conjugating olefin group instead of the hydroxy-allene group. Next, in order to understand why peridinin possesses the irregular C37 skeleton, we designed three peridinin derivatives as a series of different  $\pi$ -electron chain length compounds. These are C33 derivative **5** which has two fewer double bonds than peridinin, C35 derivative **6** which has one less double bond, and C39 derivative **7** which has one more double bond. On the other hand, in order to understand the role of the  $\gamma$ -ylidenebutenolide group, we designed the open-ring peridinin derivatives **8** and **9**. Derivative **8** possesses a triple bond and a methyl ester group, and derivative **9** has a double bond and also a methyl ester group instead of the  $\gamma$ -ylidenebutenolide group. These derivatives would provide useful information on the roles of these unique functional groups by comparing their data on the spectroscopies and energy transfer efficiencies.

According to the stereocontrolled synthesis of peridinin, which we previously established and the strategy is shown in Fig. 3 (Furuichi et al., 2002, 2004), we planned to synthesize these peridinin derivatives by a coupling between the pairs of C17-allenic segment **10** and the corresponding ylidenebutenolide-modified half-segments **15-17** or C20-ylidenebutenolide half-segment **14** and the corresponding allene-modified half-segments **11-13** using the modified Julia olefination reaction (Baudin et al., 1991, 1993) (Fig. 3). Namely, we planned to synthesize the allene modified derivatives **2** and **3** by a coupling between the corresponding allene modified half-segment **12** and **13** and C20-ylidenebutenolide half-segment **14**. Next, the syntheses of both C35 and C39 peridinin derivatives **6** and **7** would be possibly synthesized by utilizing the modified Julia olefination of the appropriate allenic

half segments such as **10** and **11** with the suitable  $\gamma$ -ylidenebutenolide half segments such as **14** and **15**, respectively. Thus, a coupling between C15-allenic segment **11** and C20-ylidenebutenolide segment **14** would produce C35 peridinin derivative **6**. Meanwhile, applying the same method to the coupling between C17-allenic segment **10** and C22-ylidenebutenolide segment **15** might produce the desired C39 peridinin derivative **7**, if the coupling product would be enough stable to be handled. On the other hand, we planned to synthesize acetylene ester derivative **8** and olefin ester derivative **9** by a coupling between the C17-allenic half-segment **10** and the corresponding ylidenebutenolide-modified half-segments **16** and **17**. We have really achieved the synthesis of these complex peridinin derivatives **2-9** by this efficient strategy.

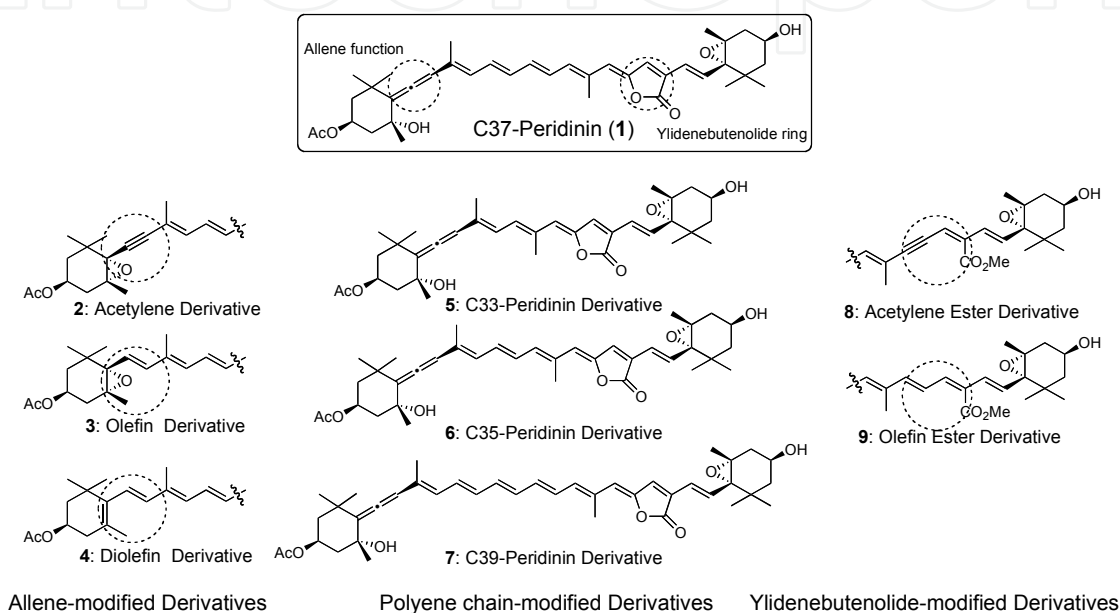


Fig. 2. Structure of peridinin and its derivatives

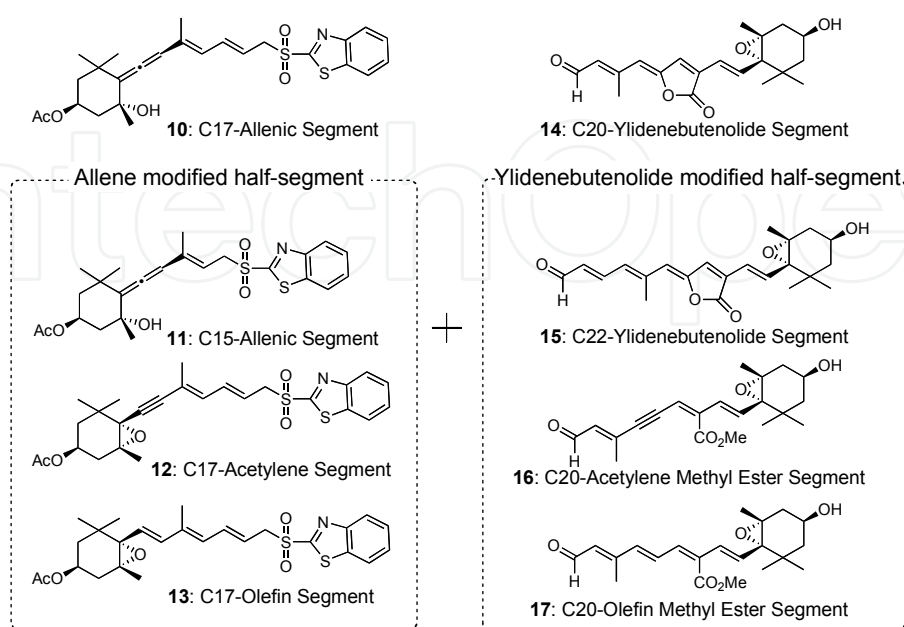


Fig. 3. Synthetic strategy



consideration; this reaction proceeded by intramolecular  $S_N2'$  hydride reduction resulting from the coordination between the oxygen atom of the epoxide in **21** and the aluminum atom of DIBAL, as shown in **22**. The obtained acetyl diol **24** was transformed into the C17-allenic segment **10** using the Mitsunobu reaction with 2-mercaptobenzothiazole, followed by oxidation of the resulting sulfide **25** with aqueous 30%  $H_2O_2$  and  $(NH_4)_6Mo_7O_{24}$ .

The terminal segments **26**, **30** and **34** were led to the each half-segment **12**, **13** and **37** shown in Fig. 4, respectively. The Sonogashira cross-coupling between **26** and vinyl iodide **27** under the same reaction condition produced the desired alcohol **28** in 80% yield. The obtained alcohol **28** was transformed into the acetylene segment **12** using the Mitsunobu reaction with 2-mercaptobenzothiazole, followed by oxidation of the resulting sulfide with aqueous 30%  $H_2O_2$  and  $Na_2WO_4 \cdot 2H_2O$ , which was milder than  $(NH_4)_6Mo_7O_{24}$  (Schulz et al., 1963).

On the other hand, the olefin segment **13** would be obtained by a coupling between vinyl iodide **30** and vinylstannane **31**. The Stille cross-coupling reaction of **30** with vinyl stannane **31** in the presence of  $PdCl_2(CH_3CN)_2$  and LiCl gave the desired alcohol **32** in excellent yield as a single isomer. The Stille cross-coupling of the opposite combination between the corresponding stannane and iodide did not afford the desired result. The alcohol **32** was transformed into sulfide **33** by the same procedure. Oxidation of **32** under the same reagent as that for the preparation of **12** gave the desired **13**. However, the use of 30%  $H_2O_2$  and  $(NH_4)_6Mo_7O_{24}$ , which is a little strict condition, gave a mixture of the desired **13** and the isomerized **13'** in low yield, and the ratio of **13** and **13'** was not reproducible (1: 4 to 1: 1). It is noteworthy that sulfone **13** was easily isomerized to **13'** by a trace amount of hydrochloric acid in  $CDCl_3$ .

Next was the synthesis of diolefin segment **37**. The Stille cross-coupling of **34** with vinyl stannane **31**, which was used in the synthesis of **13**, afforded tetraene alcohol **35** as a single isomer. In this coupling, the reaction smoothly proceeded at room temperature, and when  $iPr_2NEt$  was not used, a mixture of **35** and its 9Z-isomer was obtained in a ratio of eight to one by NMR. The amount of 9Z-isomer seemed to increase at higher reaction temperature, for instance, 9E/9Z = 3/1 at 60 °C, which is the same condition to that of the synthesis of **13**. The desired sulfone **37** was obtained from **35** by the Mitsunobu reaction with 2-mercaptobenzothiazole, followed by oxidation of the resulting sulfide with aqueous 30%  $H_2O_2$  and  $Na_2WO_4 \cdot 2H_2O$ , as a mixture of 9E/9Z = 10/1 in 31% yield. The use of 30%  $H_2O_2$  with  $(NH_4)_6Mo_7O_{24}$  and mCPBA gave a complex mixture. Oxidation of the allylic sulfide to the corresponding sulfone in longer conjugated polyenes was still problematic.

We chose the modified Julia olefination as the final C-C coupling reaction, because most of this olefination proceeded even at -78 °C. Such low temperature reaction was well suitable for the construction of the poly functionalized polyene chain such as peridinin. For instance, the crucial modified Julia olefination was explored as the final key step in the synthesis of acetylene derivative **2**. The reaction of an anion derived from **12** with **14** at -78 °C smoothly proceeded within 5 min in the dark to produce the peridinin derivatives in 42% amount as a mixture of stereoisomers. Due to the previous experiments in our carotenoid syntheses and the reports of the Brückner's and de Lera's groups that the modified Julia olefination of polyene compounds generally produced the Z-isomer at the connected double bond (Bruckner et al., 2005; Vaz et al., 2005), we tried to isomerize the connected double bond monitoring by HPLC as shown in Fig. 5. The resulting mixture was allowed to stand in benzene at room temperature under fluorescent light in an argon atmosphere. The isomerization under fluorescent light was faster than that in the dark. After 2 days, we

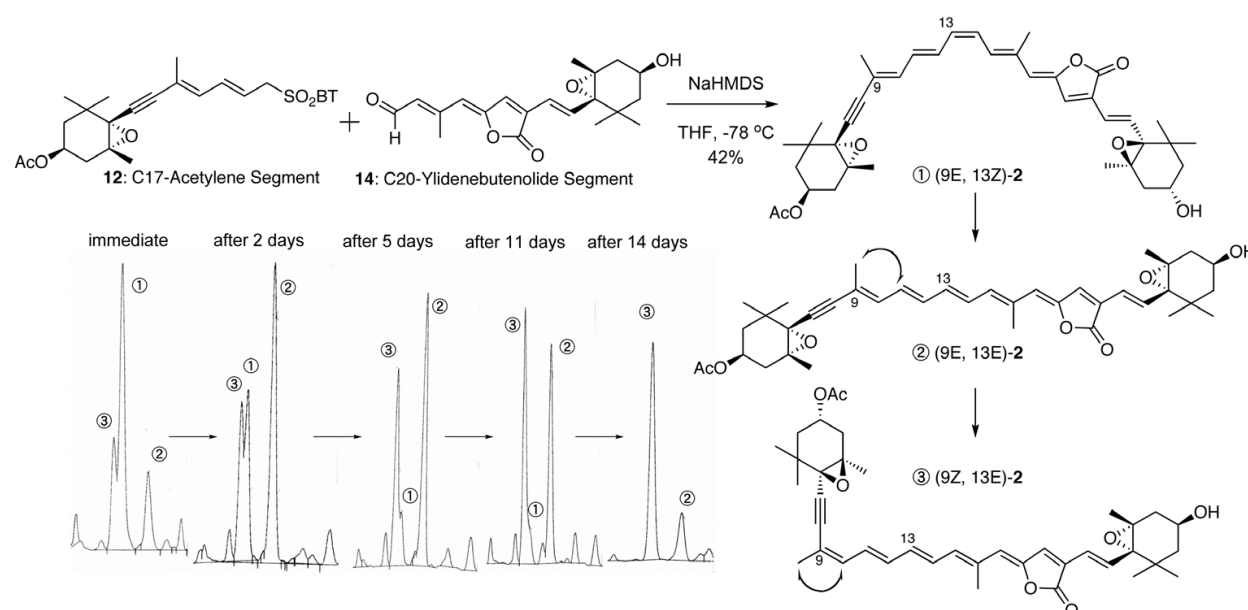


Fig. 5. Isomerization and structure of acetylene derivative

observed that the initially generated major peak (peak 1 in the immediate situation) changed to another major peak (peak 2). After 11 days, while the peak 2 gradually decreased, the peak 3 increased. After 14 days, the peak 2 became the major peak in an equilibrium state. We isolated all peaks by both the mobile-phase and the reverse-phase HPLC, and elucidated their structures by NMR (400 and 750 MHz). Thus, we clarified that the peak 1 was (9E, 13Z)-isomer **2**, the peak 2 was (9E, 13E)-all-*trans* acetylene derivative **2**, and peak 3 was (9Z, 13E)-isomer **2**. All-*trans* derivative **2** did not isomerize to the 9Z-isomer at -20 °C but gradually isomerized at room temperature in the dark. Obviously, all-*trans* isomer was unstable at room temperature and easily isomerized to the 9Z-isomer (Vaz et al., 2006), which was the most stable isomer. In addition, olefin derivative **3** and diolefin derivative **4** were synthesized by the same procedure (Kajikawa et al., 2009a).

### 2.3 Syntheses of polyene-chain modified derivatives

Next, we synthesized polyene chain modified peridinin derivatives by using a stereocontrolled domino one-pot formation of the ylidenebutenolide as a key step. First, dibromide **40** was obtained by a sequence of the Wittig reaction,  $^1\text{O}_2$  oxygenation followed by a treatment with diisopropylethylamine in the presence of allyl bromide, and the Corey's dibromination from aldehyde **38**, which was prepared from (-)-actinol in 53% for 4 steps. Dibromide **40** was successfully transformed into alkyne **41** by the treatment with TBAF in 81% yield (Tanaka et al., 1980). Next was the key stereocontrolled preparation of the ylidenebutenolide segment **14** from alkyne **41** (Fig. 6). Thus, alkyne **41** was treated with vinyl iodide **42** and cuprous iodide in triethylamine for 1 h followed by an addition of formic acid after confirming the consumption of the starting **41** by TLC analysis. The mixture was then further stirred at room temperature for overnight to produce the desired ylidenebutenolide **45** in 49% yield under the stereocontrolled fashion in one-pot. This three-step domino one-pot reaction to prepare the ylidenebutenolide **45** could be explained in detail by the possible mechanism shown in Fig. 6. At first, Sonogashira coupling of **41** and iodide **42** proceeded to afford the desired coupling product, in which the  $\pi$ -allylpalladium generated from the allylester group was formed and coordinated to the alkyne such as **43**.

Next, the intermediary **43** underwent  $\pi$ -allylalkenylpalladium(II)-assisted regio- and stereoselective intramolecular cyclization to form the  $\pi$ -allylalkenylpalladium lactone intermediate **44**. In the final step, the  $\pi$ -allylalkenylpalladium moiety was removed by hydrogenolysis with formic acid to give the desired ylidenebutenolide **45**. MnO<sub>2</sub> oxidation of **45** gave the stereocontrolled ylidenebutenolide segment **14**.

The crucial one-pot ylidenebutenolide formation from **41** and vinyl iodide **46**, which was previously synthesized by us, was explored as the key step in the synthesis of C33 peridinin derivative **5**. Thus, a mixture of **41** and **46** was stirred in the presence of catalytic amounts of Pd(PPh<sub>3</sub>)<sub>4</sub> and cuprous iodide in triethylamine at 45 °C for 10 min. After the complete consumption of **41** was ascertained by TLC, formic acid was added to the reaction mixture and then the mixture was stirred at 45 °C for 10 min to produce the desired C33 peridinin derivative in 35% yield as a mixture of stereoisomers in one-pot. The undesired 11Z-isomer **46** resulted in the undesired 11Z-isomer of the compound **5**. The resulting mixture was then allowed to isomerize in benzene at room temperature under fluorescent light in an argon atmosphere to successfully produce the desired **5** as a mixture of stereoisomers (Fig. 7).

Next, the stereocontrolled preparation of C22-ylidenebutenolide segment **15** from alkyne **41** was fortunately successful by the same procedure; a mixture of **41** and vinyl iodide **47** was stirred at 45 °C for 10 min to produce the desired ylidenebutenolide compound **15** in 40% yield as the 13'E/ 13'Z mixture (10/ 1). The reaction with the corresponding hydroxy derivative of **47** did not give the desired result because of its instability.

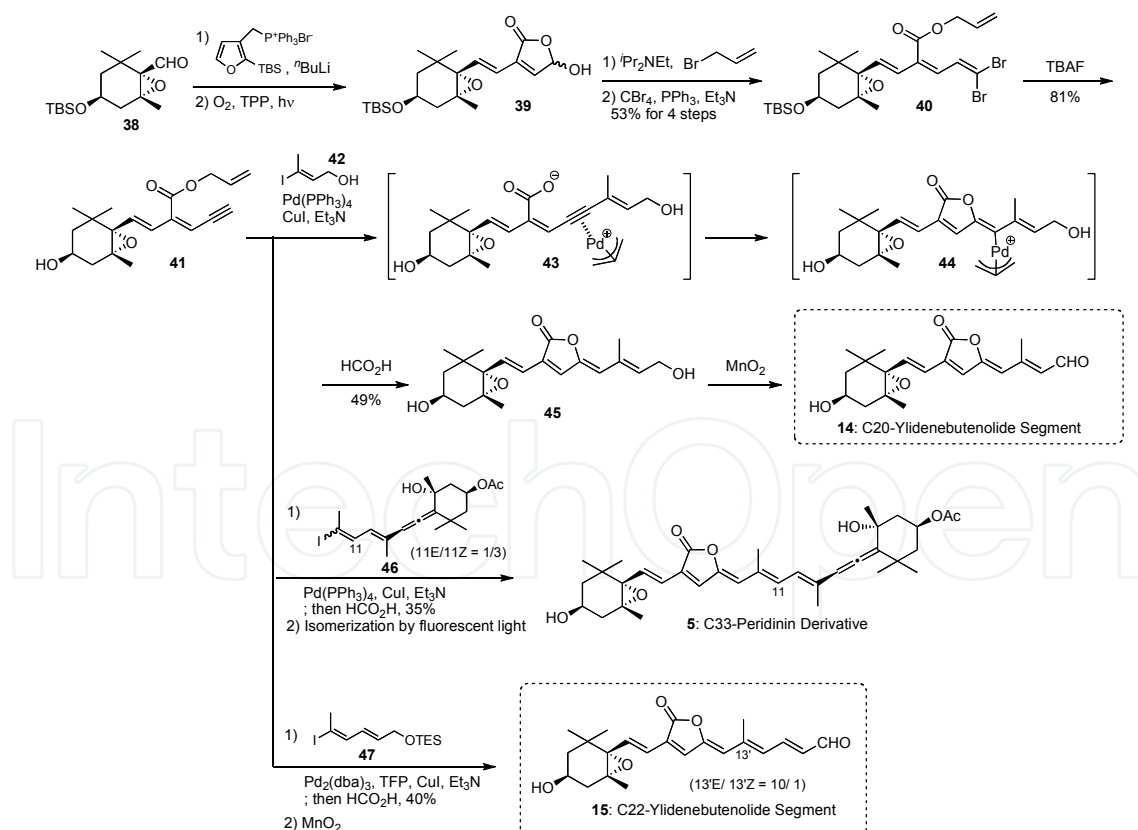


Fig. 6. Synthesis of stereocontrolled ylidenebutenolide moiety

We thus successfully synthesized the C20- and C22-ylidenebutenolide half-segments **14** and **15**, and C33 peridinin derivative **5** by the same way. The isomerization of C33 peridinin

derivative was shown in Fig. 7 (A). The resulting mixture was then allowed to isomerize in benzene at room temperature under fluorescent light in an argon atmosphere. After 2 days, we observed that the initially generated major peak (peak 2) in Fig. 7 (A) changed into another major peak (peak 1) in the HPLC. In addition, peak 3 became larger after 2 days, when the situation would be an equilibrium state. We isolated all peaks by the mobile-phase HPLC and elucidated their structures by NMR (400 MHz), and we elucidated that peak 1 was fortunately (11E, 11'Z)-all-*trans* C33 peridinin **5**, peak 2 was (11Z, 11'Z)-isomer **5'** and peak 3 was (11E, 11'E)-isomer **5''**, respectively. Interestingly, (11E, 11'E)-isomer **5''** was the secondarily larger isomer in the equilibrium state.

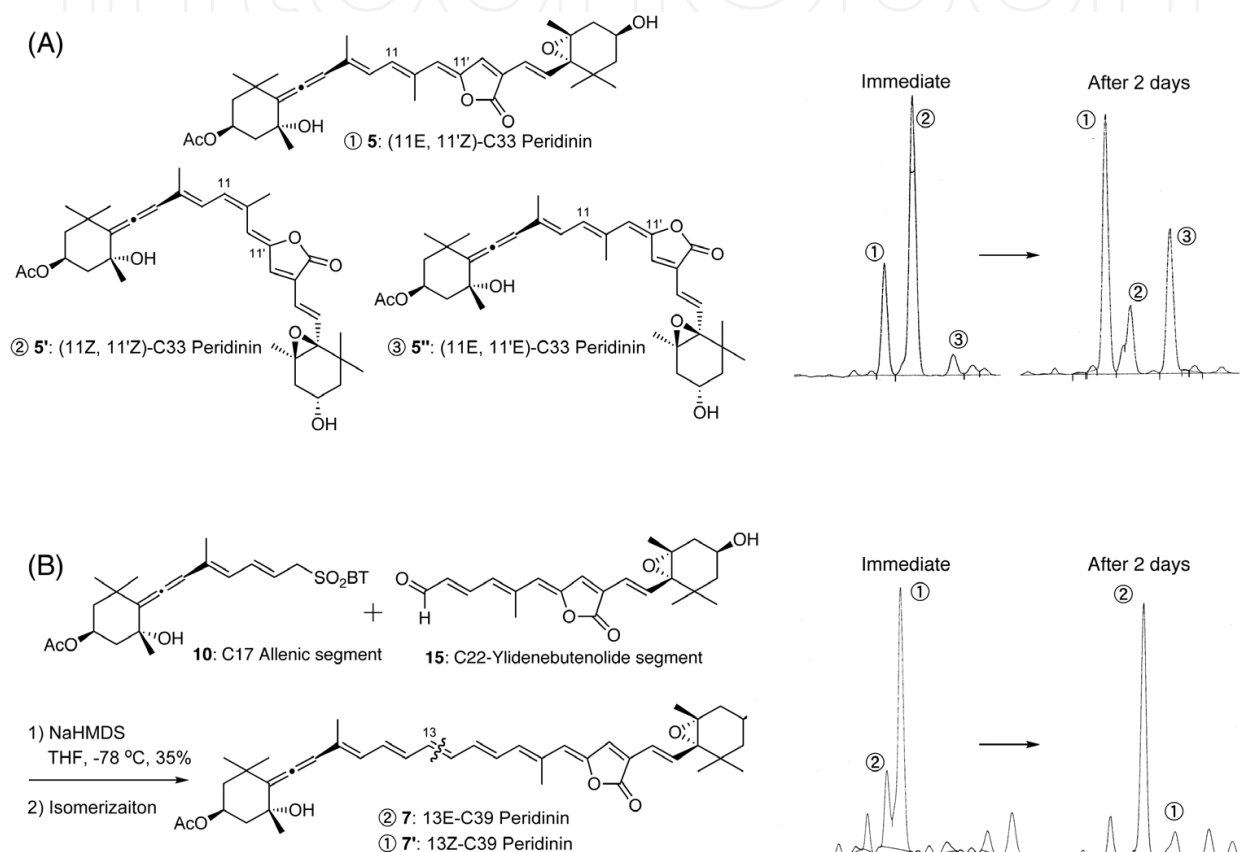


Fig. 7. Structure and HPLC analysis of (A) C33 and (B) C39 peridinin derivatives

Furthermore, relatively unstable C39 peridinin derivative **7** was synthesized by the same protocol as shown in Fig. 7 (B). Thus, the anion derived from **10**, which was the allenic half-segment of the established peridinin synthesis (Fig. 3), was stirred with **15** under the same condition. Fortunately, the reaction completed within 5 min in the dark to produce the coupling products as a mixture of the stereoisomers in almost 35% amount, in which the 13Z-isomer (peak 1) was estimated to be 48% of the mixture by HPLC analysis (13E-isomer: peak 2 was 19%). Isomerization to the desired **7** was again attempted by the same method. After 2 days, a large amount of the 13Z-isomer **7'** (peak 1) changed to the all-*trans* C39 peridinin derivative **7** (peak 2) (57% based on HPLC analysis) in an equilibrium state. We then isolated both compounds, and confirmed their structures by NMR (400 and 750 MHz). The synthesized all-*trans* C39 peridinin derivative gradually decomposed within one month under an argon gas atmosphere at around  $-20^{\circ}\text{C}$ . This instability was in good contrast to the

case of peridinin, which could be stored without any remarkable decomposition under the same conditions. Meanwhile, C35 peridinin derivative was also synthesized by the same procedure (Kajikawa et al., 2009b).

#### 2.4 Syntheses of ylidenebutenolide modified derivatives and the stereochemical and spectral characteristics of the synthesized derivatives

Finally, the synthesis of ylidenebutenolide modified peridinin derivatives is described. The acetylene ester derivative was synthesized by the same protocol. Namely, the coupling between C17-allenic segment **10** and C20-acetylene methyl ester segment **16** by using the modified Julia olefination, which was followed by the isomerization gave all-*trans* **8** (Fig. 8 (A)) (Kajikawa et al., 2010).

On the other hand, there were some difficulties in the synthesis of the olefin ester derivative (Fig. 8). We obtained the only 9'E-olefin ester segment **17** by the similar synthetic process, which was not the desired 9'Z half-segment resulting from the contribution of the carbonyl group of the methyl ester. We then tried to connect the segments **10** and **17** by the modified Julia olefination and to obtain all-*trans* **9-3** by the isomerization. The anion derived from **10** was stirred with a mixture of stereoisomers of **17** under the same conditions used for the coupling of the previous peridinin derivatives. The reaction was completed within 5 min in the dark to produce the coupling products as a mixture of the stereoisomers in 46% amount, whose HPLC is shown in Fig. 8 (B). The major peak (peak 1) was estimated to be 45% of the mixture by HPLC analysis (other isomers were 16%, 14%, 5%, 5%, and others). Isomerization to the desired all-*trans* **9-3** was attempted under the same conditions previously used. After 5 days, the initially generated major peak (peak 1) changed to another peak (peak 2; 44% based on HPLC analysis) in an equilibrium state. We then isolated both compounds and elucidated their structures by NMR (400 and 750 MHz), and clarified that peak 1 was (13Z, 9'E)-isomer **9-1** and peak 2 was (13E, 9'E)-isomer **9-2**. Unfortunately, we could not obtain the desired all-*trans* (13E, 9'Z)- isomer **9-3**.

We investigated the stability of the synthesized ring opened derivatives **8** and **9**, and found the isolated all-*trans* acetylene ester derivative **8-1** was more labile than **8-2** (13Z-isomer). For instance, the isolated all-*trans* derivative **8-1** (13E-isomer) isomerized to the dihydrofuran derivative **8'** by a trace amount of hydrogen chloride in CDCl<sub>3</sub>, but the corresponding isomerization of **8-2** (13Z-isomer) was not observed (Fig. 8). In addition, the all-*trans* derivative **8-1** rapidly isomerized to give a mixture of Z-isomers upon illumination. This might occur due to the contribution of the carbonyl group of the methyl ester similar to the case of the 9'E-olefin ester derivative **9-2**.

In the PCP complex, peridinin exhibits an exceptionally high efficiency of energy transfer to Chl a. In order to make clear the effect of the ylidenebutenolide, we needed to measure the energy transfer efficiencies in peridinin derivatives. Furthermore, it was tried to construct the corresponding PCP derivatives using the synthesized peridinin derivatives **8** and **9** to compare with the energy transfer efficiencies of peridinin (private information from Dr. H. A. Frank). First, it was attempted to reconstitute the PCP apoprotein using the 9'E-olefin ester derivative **9-2** under the same conditions that were successful for peridinin (Ilagan et al., 2006), but the reconstitution was not observed. It was also tried to reconstitute the PCP apoprotein using the 13Z-isomer **8-2**, but it did not bind the protein either. The reason might be that these compounds were bent into a *cis* configuration, and hence they might not fit properly into the protein binding site. These results apparently showed that the  $\gamma$ -ylidenebutenolide of peridinin at least contributes to the stereochemical stability of the

compound and would keep the all-*trans* conformer suitable for incorporation into the protein to form the PCP complex.

The maximum absorption wavelengths ( $\lambda_{\max}$ ) in the electronic spectra of peridinin (**1**) and the synthesized derivatives **2**~**7**, **8-1** and **9-2** in hexane were measured and are summarized in Fig. 9. Evidently, the diolefin derivative **4** and C39 peridinin derivative **7** showed the longer  $\lambda_{\max}$  than that of peridinin. The  $\lambda_{\max}$  value in polyene chain modified derivatives **5**~**7** increased almost 20 nm per one olefin unit added to the conjugated polyene. On the other hand, the olefin derivative **3**, having eight conjugated carbon-carbon double bonds like peridinin, showed the shorter  $\lambda_{\max}$  than that of peridinin. The open-ring derivative also displayed a shorter  $\lambda_{\max}$  than peridinin (**1**) due to shorter effective  $\pi$ -electron conjugated chain length, although the 9'*E*-olefin ester derivative **9-2** had the same conjugated carbon-carbon double bonds compared with peridinin. These results show that the allene and ylidenebutenolide group at least contribute to giving rise to the  $\lambda_{\max}$  value desirable for the marine organism to absorb light in the blue-green region of the visible spectrum.

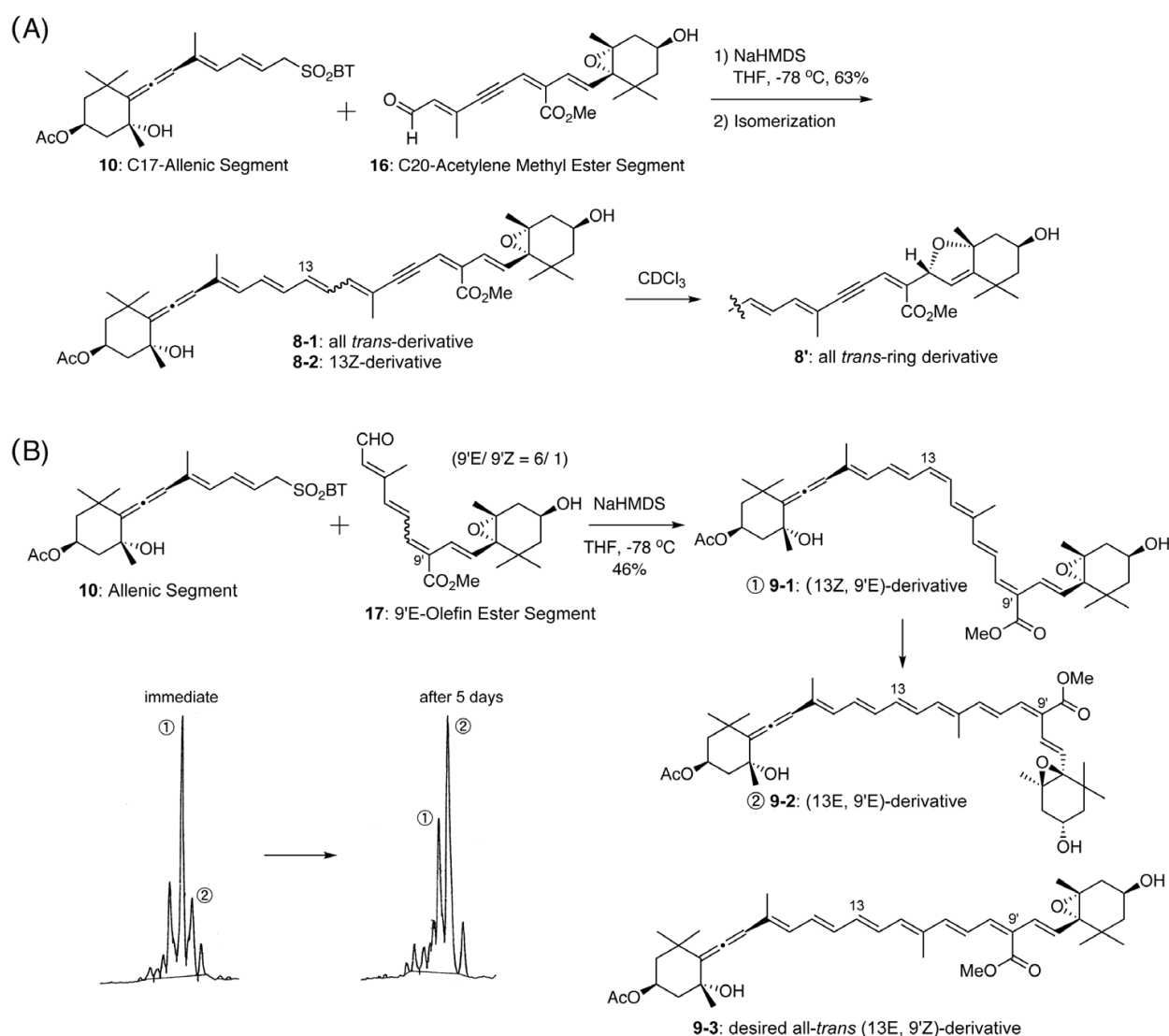


Fig. 8. Stereochemical characteristics of ylidenebutenolide modified derivatives

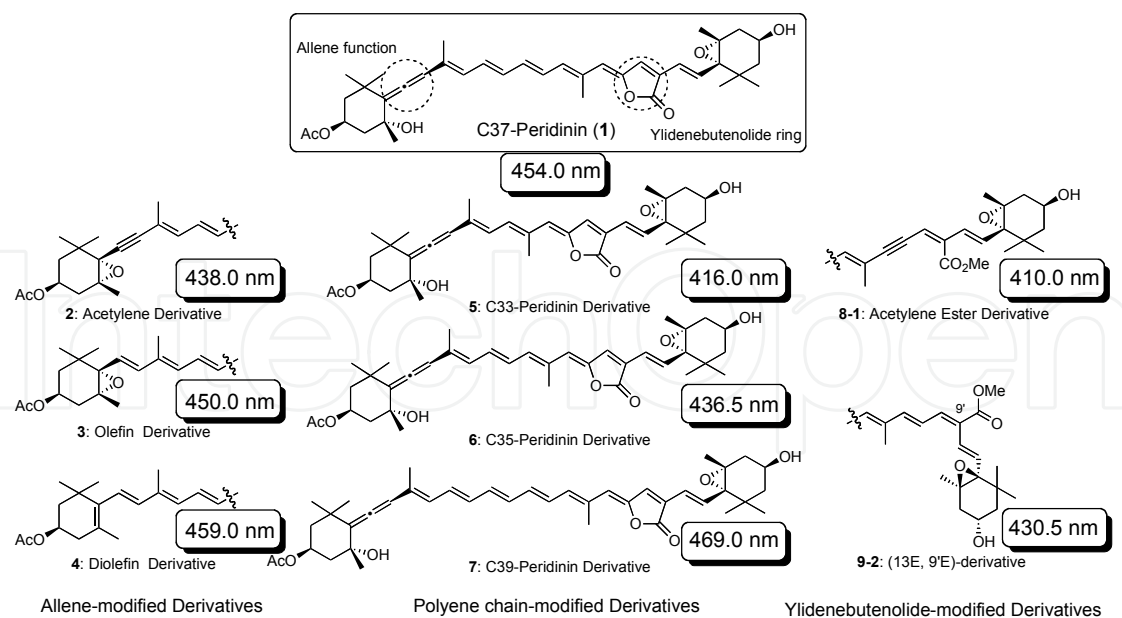


Fig. 9. Structure of synthesized peridinin derivatives and result of UV spectra in hexane

### 3. Relationships between the unique structure and the special excited state of peridinin

#### 3.1 Measurement of ultrafast time-resolved optical absorption spectra

From studies on peridinin and other carotenoids, it has been known that there are at least two important low-lying excited singlet states, denoted  $S_1$  and  $S_2$ , which are related to the highly efficient energy transfer from peridinin to chlorophyll a (Fig. 10(A)). To elucidate the mechanism of this efficient energy transfer, it is important that we make clear the characteristics of these excited states and the energy transfer pathways such as those from  $S_2$  to  $Q_X$  and/or from  $S_1$  to  $Q_Y$ . Recently, many researchers have tried to examine this particular mechanism. The conjugated double bonds of most carotenoids are symmetry and these double bonds can be regarded as polyenes described in terms of the idealized  $C_{2h}$  point group in the spectroscopic fields (Hudson et al., 1973). The lowest excited singlet ( $S_1$ ) state is assigned to the  $2^1A_g^-$  state, and the second lowest singlet ( $S_2$ ) state is assigned to the  $1^1B_u^+$  state. The excitation to  $S_1$  from the ground state is symmetry forbidden and is not directly accessible by one-photon processes in contrast to the allowed absorption to  $S_2$  state (Polivka et al., 2004). On the other hand, the conjugated double bond of peridinin and other carbonyl-containing carotenoids are asymmetric due to the presence of the conjugated carbonyl group, and these oxygenated carotenoids display a pronounced solvent dependence of its lowest excited singlet state lifetime ( $S_1$  lifetime). Namely, it has been proposed that the findings are consistent with the presence of an intramolecular charge transfer (ICT) state, which is uniquely formed in carotenoids containing the carbonyl group in conjugation with the  $\pi$ -electron system of double bonds (Frank et al., 2000; Zigmantas et al., 2004). It has also been argued that changes in the position of the ICT state related to the  $S_1$  state rationalize the dependence on solvent polarity concerning  $S_1$  lifetime. In the case of peridinin, the relationship of these energy levels is well discussed based on the detailed experimental works. The ICT in the excited state manifold of peridinin is shown to be higher in energy than the  $S_1$  state in nonpolar solvents and shifts below  $S_1$  with increasing solvent polarity

(Bautista et al., 1999) (Fig.10 (B)). In addition, it is suggested that the efficient energy transfers are related with this ICT state. Proposals for the nature of the ICT state include its being a separate electronic state from  $S_1$  (Vaswani et al., 2003; Papagiannakis et al., 2005), quantum mixed with  $S_1$  (Shima et al., 2003) or simply  $S_1$  itself. Although there are many discussions with experiments and calculations, the precise nature of the ICT state remains to be elucidated. Under these back-ground on the proposed attractive energy level, ICT energy level, a new approach, that the synthesis of a series of peridinin analogues followed by their spectroscopic measurements are investigated, has been started as a collaboration work between Connecticut University, Osaka City University and Kwansei Gakuin University of Hyogo. Thus, to explore the nature of the ICT state in carbonyl-containing carotenoids, both steady-state and ultrafast time resolved optical spectroscopy have been performed on peridinin and its synthetic derivatives.

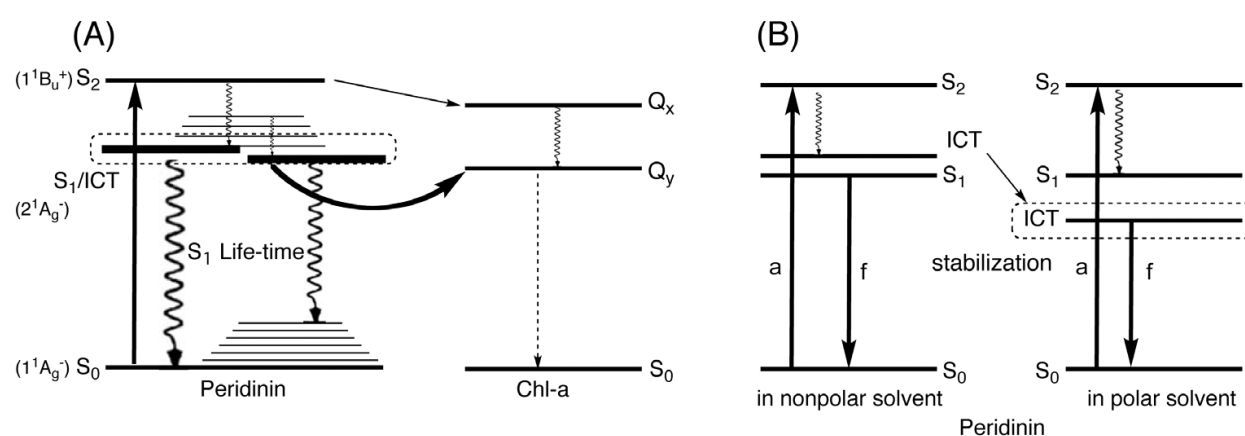


Fig. 10. (A) Energy transfer from peridinin to chl-a and (B) the nature of ICT state

The ultrafast time resolved optical absorption experiments of peridinin (**1**) and many other carbonyl-containing natural carotenoids such as fucoxanthin and spheroidenone were measured, and their  $S_1$  lifetimes were reported by the analysis of their ultrafast time resolved optical absorption (Frank et al., 2000). The lifetime of three natural carotenoid was reported to depend on the polarity of the measured solvents, and this effect is attributed to the presence of an intramolecular charge transfer (ICT) state in the manifold of the excited states of these molecules. We then measured the lifetime of the lowest excited single state of the four compounds, which are C33, C35 and C39 synthesized derivatives along with peridinin, and the results are listed in Fig. 11 (A). The data listed in Fig. 11 (A) show that the lifetime is shorter in the polar solvent, methanol, and is longer in a non-polar solvent, *n*-hexane. This means that the ICT states in the excited state manifold of peridinin and its three derivatives are higher energy than the  $S_1$  state in nonpolar solvents, and they shift to a lower energy than the  $S_1$  state in polar solvents. These experiments on peridinin and its derivatives revealed an increasing solvent effect with the decreasing  $\pi$ -electron chain length. This result agrees with the experimental results carried out on conjugated apo-carotenoids (Ehlers et al., 2007). The lifetime of the lowest excited singlet state of C33 peridinin derivative **5** is the one most strongly dependent on the solvent polarity. In fact, this is the strongest solvent dependence on the lifetime of the carotenoid excited state so far yet reported. Moreover, the most striking observation in the data is that the lifetime of the ICT state converges to a value of  $10 \pm 1$  ps in the polar

solvent, methanol, for all the peridinin analogues regardless of the extent of  $\pi$ -electron conjugation. Potential energy level diagrams for four molecules in polar and nonpolar solvents are described as shown in Fig. 11 (B). Based on the results of  $S_1$  lifetime, although  $S_1$  state gradually drops as longer polyene chain in hexane, the ICT state exists in the same position in methanol. We dramatically observed that the behavior of ICT states were obviously different from that of  $S_1$  states in the series of our synthesized peridinin derivatives including peridinin itself. These results strongly support the idea that the  $S_1$  and ICT states act as independent states. We can not, however, conclude clearly whether ICT state is separate or mixed energy level from  $S_1$  state. The unexpected phenomena, that the ICT state exists in the same position in methanol, is quite interesting. We can presume that this nature of the ICT state is very important for energy transfers because the environment in methanol is considered to be the nearly same to that of PCP complex (Akimoto et al., 1996).

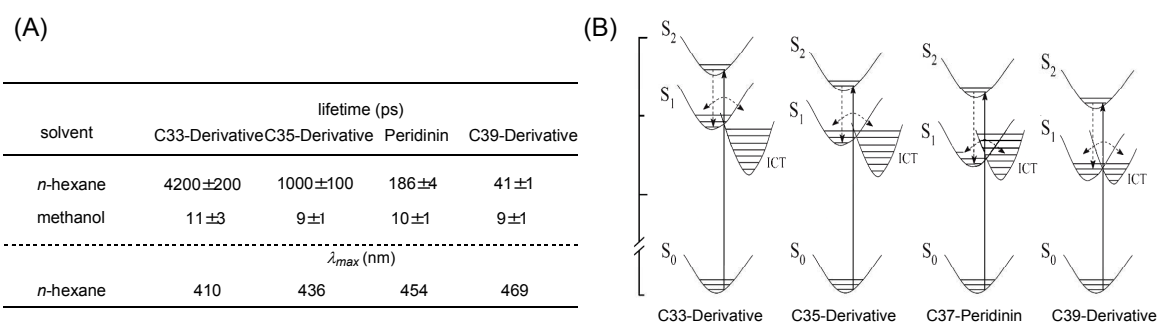


Fig. 11. (A) Result of  $S_1$  lifetime and (B) proposed energy level diagram

### 3.2 Measurement of Stark spectra

The precise relationship between  $S_1$  and ICT energy levels and also the nature of ICT are described in the previous chapter. On the other hand, there has also been a suggestion of the relationship between  $S_2$  and ICT states. The measurement of electroabsorption spectroscopy (Stark spectra) of peridinin has been reported (Premvardhan et al., 2005). Stark spectra can determine the change in electrostatic properties and estimate the change of the static dipole moment ( $|\Delta\mu|$ ) between in the ground state and in the excited state. Thus, the value of this change represents by  $|\Delta\mu|$ . Based on the observation, it is found that the absorption band from  $S_0$  to  $S_2$  shows large static dipolemoment change. In addition, it is suggested that in PCP complex there may be strong dipole-dipole coupling between peridinin and chlorophyll a. The large dipole moment would allow for strong dipolar interaction between peridinin and Chl a in PCP, and would contribute to high energy transfer. It has also been recently proposed that the presence of the ICT excited state promotes dipolar interactions with Chl a in the PCP complex and facilitates energy transfer via a dipole mechanism (Zigmantas et al., 2002). Although the magnitude of the static dipole moment is suggested to be very important, the relationship between the structural features of peridinin and the dipole moment has not been made clear. We then measured the Stark absorption spectra of peridinin along with its allene modified and polyene chain modified derivatives. Stark spectra is particularly suitable for peridinin and its derivatives, because the presence of the ICT state would be directly discernible.

The Stark spectra and the maximum absorption of the electronic spectra of peridinin (1) and the synthesized derivatives (2-4, 6 and 7) are summarized in Fig. 12. The Stark spectra of

peridinin, allene modified and polyene chain modified derivatives were recorded in methyl methacrylate polymer at 77 K. The  $|\Delta\mu|$  values were corresponding to the CT absorption band. As the results of peridinin and allene modified derivatives, peridinin showed the largest  $|\Delta\mu|$  value among all of them. Namely, peridinin yielded a  $|\Delta\mu|$  value of  $5.42 (x 10^{-29} \text{ C} \cdot \text{m})$ , acetylene derivative **2** showed 2.47, olefin derivative **3** showed 4.22, and diolefin derivative **4** showed 4.25. A  $|\Delta\mu|$  value of peridinin was in agreement with a reported value (Premvardhan et al., 2005). The  $|\Delta\mu|$  value generally shows a larger number with the increasing  $\pi$ -electron chain length theoretically. Although peridinin possesses fewer conjugating double bonds and shows a shorter  $\lambda_{\text{max}}$  rather than that of diolefin derivative **4**, the  $|\Delta\mu|$  value of peridinin was the largest among the four compounds. The difference in the  $|\Delta\mu|$  value is evidently attributable to the difference in the functional groups. Thus, we have understood that the unique allene group contributes to production of the large dipole moment in the molecule. These results strongly suggest that the allene group of peridinin is essential for formation of the effective ICT state, which would allow the quantitative energy transfer to Chl a in the PCP complex. This is the first experimental evidence that shows the allene group in peridinin enhances the ICT character (Kusumoto et al., 2010).

In addition, as the results of peridinin and polyene chain modified derivatives, peridinin (**1**) also showed the largest  $|\Delta\mu|$  value among all of them. Namely, peridinin (**1**) yielded a  $|\Delta\mu|$  value of  $5.42 (x 10^{-29} \text{ C} \cdot \text{m})$ , C35 peridinin derivative **6** showed 4.25, and C39 peridinin derivative **7** did 5.29. The  $|\Delta\mu|$  value generally shows a larger number with the increasing  $\pi$ -electron chain length (Kajikawa et al., 2009b). Although peridinin possesses fewer conjugated double bonds and shows a rather shorter  $\lambda_{\text{max}}$  than that of C39 peridinin derivative **7**, the  $|\Delta\mu|$  value of peridinin (**1**) was the largest among the three compounds. Thus, the C37 skeleton of peridinin (**1**) would also contribute to the large dipole moment of the molecule in the excited state to facilitate energy transfer. This would be at least a partial answer to the question of why peridinin (**1**) possesses the irregular C37 skeleton.

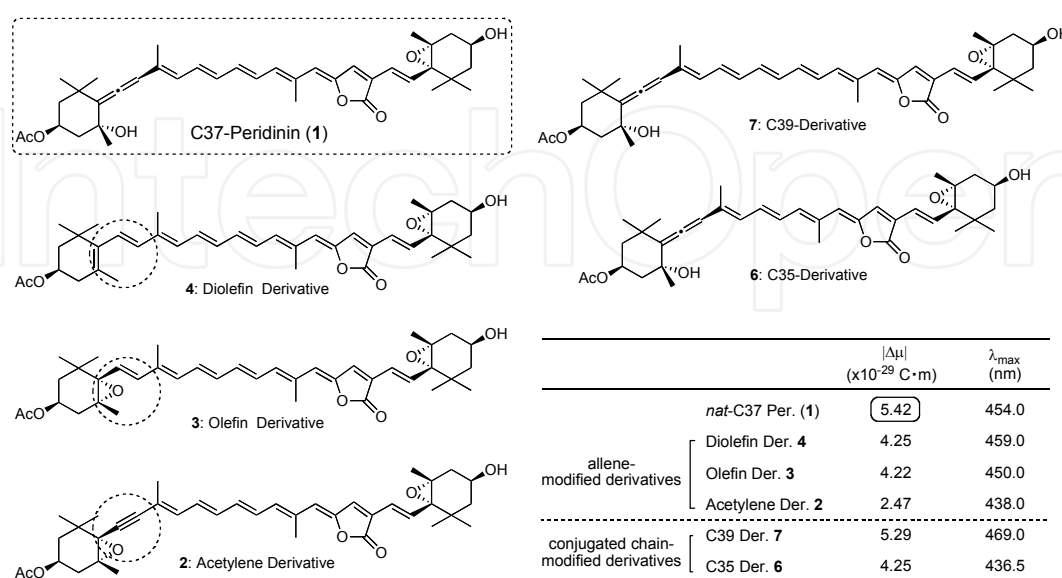


Fig. 12. Structure of Peridinin and its derivatives and the result of Stark spectra

#### 4. Conclusion

The research on the efficient energy transfer mechanism of the primary photochemical events of photosynthesis have been exactly developed by the new approach based on the synthetic organic chemistry. Namely, the relationship between the characteristic structure of peridinin and the nature of its ICT state has been gradually made clear by synthesizing a series of peridinin analogues and comparing their characteristics to those of peridinin.

Stark spectra of peridinin, allene modified, and polyene chain modified derivatives have showed that the dipole moment of the excited state ( $|\Delta\mu|$  value) of peridinin is the largest among the series of six compounds, although the increasing  $\pi$ -electron chain length generally shows a larger value of  $|\Delta\mu|$ . These results apparently show that the allene group and C37 skeleton of peridinin effectively contributes to production of the large dipole moment in the molecule in excited state, which would result in the high energy transfer efficiencies to Chl a in the PCP complex. This is an answer of why peridinin possesses the unique allene bond and the irregular C37 skeleton.

In addition, the ultrafast time resolved optical absorption spectra of polyene chain modified derivatives including peridinin show that the lifetime of the lowest excited singlet state of C33 peridinin derivative has the strongest solvent dependence so far yet reported. Furthermore, the data reveal the striking observation that the lifetime of the ICT state converges to a value of  $10 \pm 1$  ps in methanol for all peridinin analogues regardless of the extent of  $\pi$ -electron conjugation. These data strongly support the notion that the  $S_1$  and ICT states behave independently.

On the other hand, comparing the stereochemical stability and spectral characteristics of the synthesized ylidenebutenolide modified analogues to those of peridinin has resulted in the conclusion that this particular functional group at least contributes to maintaining the stereochemistry of the conjugated double bonds in the all-*trans* configuration and giving rise to a  $\lambda_{\max}$  value desirable for the marine organism to absorb light in the blue-green region of the visible spectrum.

These inherent characteristics of peridinin are important clues for elucidating the energy transfer mechanism from the light-harvesting carotenoids to chlorophylls. The studies to measure the energy transfer efficiencies of peridinin derivatives are currently in progress to further understand the exact role of these unique functional groups.

#### 5. Acknowledgment

We thank Dr. Thomas Netscher of DSM Nutritional Products, Ltd., for the donation of (-)-actinol **18**. We also would like to thank Prof. H. A. Frank (University of Connecticut) with ultrafast experiments and Prof. H. Hashimoto (Osaka City University) with Stark spectra measurement. This work was supported by a Grant-in-Aid for Science Research on Priority Areas 16073222 from the Ministry of Education, Culture, Sports, Science and Technology, and Matching Fund Subsidy for a Private University, Japan. T. K. is also grateful for receiving the Scholar Ship of JSPS.

#### 6. References

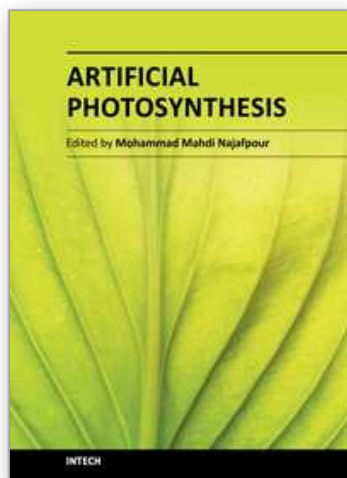
Akimoto, S.; Takaichi, S.; Ogata, T.; Nishiyama, Y.; Yamazaki, I. & Mimuro, M. (1996). Excitation energy transfer in carotenoid chlorophyll protein complexes probed by

- femtosecond fluorescence decays. *Chemical Physics Letters*, 260, 1-2 (September 1996), pp. 147-152 ISSN 0009-2614
- Baudin, J. B.; Hareau, G.; Julia, S. A. & Ruel, O. (1991). A direct synthesis of olefin by reaction of carbonyl-compounds with lithioderivatives of 2-[alkyl-sulfonyl or (2'-alkenyl)-sulfonyl or benzyl-sulfonyl]-benzothiazoles. *Tetrahedron Letters*, 32, 9 (February 1991), pp. 1175-1178 ISSN 0040-4039
- Baudin, J. B.; Hareau, G.; Julia, S. A. & Ruel, O. (1993). Stereochemistry of direct olefin formation from carbonyl-compounds and lithiated heterocyclic sulfones. *Bulletin de la Societe Chimique de France*, 130, 6 (February 1993), pp. 856-878 ISSN 0037-8968
- Bautista, J. A.; Connors, R. E.; Raju, B. B.; Hiller, R. G.; Sharples, F. P.; Gosztola, D.; Wasielewski, M. R. & Frank, H. A. (1999). Excited state properties of peridinin: observation of a solvent dependence of the lowest excited singlet state lifetime and spectral behavior unique among carotenoids. *Journal of Physical Chemistry B*, 103, 41 (October 1999), pp. 8751-8758 ISSN 1089-5647
- Bruckner, R. & Sorg, A. (2005). Unexpected cis-selectivity in (Sylvestre) Julia olefination with  $\text{Bu}_3\text{Sn}$ -containing allyl benzothiazolyl sulfones: Stereoselective synthesis of 1,3-butadienyl- and 1,3,5-hexatrienylstannanes *Synlett*, 2, (February 2005), pp. 289-293 ISSN 0936-5214
- Ehlers, F.; Wild, D. A.; Lenzer, T. & Oum, K. (2007). Investigation of the  $S_1/ICT$  to  $S_0$  internal conversion lifetime of 4'-apo- $\beta$ -caroten-4'-al and 8'-apo- $\beta$ -caroten-8'-al: dependence on conjugation length and solvent polarity. *Journal of Physical Chemistry A*, 111, 12 (March 2007), pp. 2257-2265 ISSN 1089-5639
- Frank, H. A.; Bautista, J. A.; Josue, J.; Pendon, Z.; Hiller, R. G.; Sharples, F. P.; Gosztola, D. & Wasielewski, M. R. (2000). Effect of the solvent environment on the spectroscopic properties and dynamics of the lowest excited states of carotenoids. *Journal of Physical Chemistry B*, 104, 18 (May 2000), pp. 4569-4577 ISSN 1089-5647
- Furuichi, N.; Hara, H.; Osaki, T.; Mori, H. & Katsumura, S. (2002). Highly efficient stereocontrolled total synthesis of the polyfunctional carotenoid peridinin. *Angewandte Chemie-International Edition*, 41, 6, (November 2001), pp. 1023-1026, ISSN 1433-7851
- Furuichi, N.; Hara, H.; Osaki, T.; Nakano, M.; Mori, H. & Katsumura, S. (2002). Stereocontrolled total synthesis of a polyfunctional carotenoid, peridinin. *Journal of Organic Chemistry*, 69, (July 2004), pp. 7949-7959, ISSN 0022-3263
- Hofmann, E.; Wrench, P. M.; Sharples, F. P.; Hiller, R. G.; Welte, W. & Diederichs, K. (1996). Structural basis of light harvesting by carotenoids: Peridinin-chlorophyll-protein from *Amphidinium carterae*. *Science*, 272, 5269, (June 1996), pp. 1788-1791, ISSN 0036-8075
- Hudson, B. S. & Kohler, B. E. (1973). Polyene spectroscopy: The lowest energy excited singlet state of diphenyloctatetraene and other linear polyenes. *The Journal of Chemical Physics*, 59, 9, (April 1973), pp. 4984-5002
- Ilagan, R. P.; Chapp, T. W.; Hiller, R. G.; Sharples, F. P.; Polivka T. & Frank, H. A. (2006). Optical spectroscopic studies of light-harvesting by pigment-reconstituted peridinin-chlorophyll-proteins at cryogenic temperatures. *Photosynthesis Research*, 90, 1, pp. 5-15 ISSN 0166-8595
- Kajikawa T.; Aoki K.; Singh R. S.; Iwashita T.; Kusumoto T.; Frank H. A.; Hashimoto H. & Ilagan, Katsumura S. (2009). Syntheses of allene-modified derivatives of peridinin

- toward elucidation of the effective role of the allene function in high energy transfer efficiencies in photosynthesis. *Organic & Biomolecular Chemistry*, 7, 18, pp. 3723-3733 ISSN 1477-0520
- Kajikawa T.; Hasegawa S.; Iwashita T.; Kusumoto T.; Hashimoto H.; Niedzwiedzki D. M.; Frank H. A. & Katsumura S. (2009). Syntheses of C33-, C35- and C39-Peridinin and their Spectral Characteristics. *Organic Letters*, 11, 21, (November 2009), pp.5006-5009 ISSN 1523-7060
- Kajikawa T.; Aoki K.; Iwashita T.; Niedzwiedzki D. M.; Frank H. A. & Katsumura S. (2010). Syntheses of ylidenbutenolide-modified derivatives of peridinin and their stereochemical and spectral characteristics. *Organic & Biomolecular Chemistry*, 8, 11, pp. 2513-2516 ISSN 1477-0520
- Kusumoto T.; Horibe T.; Kajikawa T.; Hasegawa S.; Iwashita T.; Cogdell R. J.; Birge R. R.; Frank H. A.; Katsumura S. & Hashimoto H. (2010). Stark Absorption Spectroscopy of Peridinin and Allene-Modified Analogues. *Chemical Physics*, 373, 1-2, (July 2010), pp. 71-79 ISSN 0301-0104
- Mimuro, M.; Nishimura, Y.; Takaichi, S.; Yamano, Y.; Ito, M.; Nagaoka, S. Yamazaki, I. Katoh, T. & Nagashima, U. (1993). The effect of molecular structure on the relaxation processes of carotenoids containing a carbonyl group, *Physics letters*, 213, 5-6, (October 1993), pp. 576-580 ISSN 0009-2614
- Papagiannakis, E.; Larsen, D. S.; van Stokkum, I. H. M.; Vengris, M.; Hiller, R. G. & van Grondelle, R. Resolving the excited state equilibrium of peridinin in solution. *Biochemistry*, 43, 49, (December 2004), pp.15303-15309 ISSN 0006-2960
- Polivka, T. & Sundstrom, V. (2004). Ultrafast dynamics of carotenoid excited states: From solution to natural and artificial systems. *Chemical Reviews*, 104, 4, (April 2004), pp. 2021-2071 ISSN 0009-2665
- Premvardhan, L.; Papagiannakis, E.; Hiller, R. G. & Grondelle, R. V. (2005). The charge-transfer character of the  $S_0$  to  $S_2$  transition in the carotenoid peridinin is revealed by stark spectroscopy. *Journal of Physical Chemistry B*, 109, 32, (August 2005), pp. 15589-15597 ISSN 1520-6106
- Schulz, H. S.; Freyermuth, H. B. & Buc, S. R. (1963). New catalysts for the oxidation of sulfides to sulfones with hydrogen peroxide, *Journal of Organic Chemistry*, 28, (April 1960), pp. 1140-1142
- Shima, S.; Ilagan, R. P.; Gillespie, N.; Sommer, B. J.; Hiller, R. G.; Sharples, F. P.; Frank, H. A. & Birge, R. R. (2003). Two-photon and fluorescence spectroscopy and the effect of environment on the photochemical properties of peridinin in solution and in the peridinin-chlorophyll-protein from *Amphidinium carterae*, *Journal of Physical Chemistry A*, 107, 40, (October 2003), pp. 8052-8066 ISSN 1089-5639
- Song, P. S.; Koba, P.; Prezelin, B. B. & Haxo, F. T. (1976). Molecular topology of photosynthetic light-harvesting pigment complex, peridinin-chlorophyll-a-protein, from marine dinoflagellates, *Biochemistry*, 15, 20, pp. 4422-4427 ISSN 0006-2960
- Stain H.; Svec, W. A.; Aitzetmuller, K.; Grandolfo, M.C.; Katz, J. J.; Kjoson, H.; Norgard, S.; Liaaen-Jensen, S.; Haxo, F. H.; Wegfahrt, P. & Rapoport, H. (1971). Structure of peridinin, the characteristic dinoflagellate carotenoid. *Journal of the American Chemical Society*. 93, 7, (April 1971), pp. 1823-1825

- Tanaka, R.; Zheng, S. Q.; Kawaguchi, K.; Tanaka, T. (1980). Nucleophilic-attack on halogeno(phenyl)acetylenes by halide-ion. *Journal of the Chemical Society Perkin Transactions 2*, 11, pp.1714-1720 ISSN 0300-9580
- Vaz, B.; Alvarez, R.; Souto, J. A. & de Lera, A. R. (2005).  $\gamma$ -Allenyl allyl benzothiazole sulfonyl anions undergo cis-selective (Sylvestre) Julia olefinations, *Synlett*, 2, (February 2005), pp. 294-298 ISSN 0936-5214
- Vaz, B.; Dominguez, M.; Alvarez, R. & de Lera, A. R. (2006). The Stille reaction in the synthesis of the C37-norcarotenoid butenolide pyrrhoxanthin. Scope and limitations. *Journal of Organic Chemistry*, 71, 16, (August 2006), pp. 5914-5920 ISSN 0022-3263
- Zigmantas, D.; Hiller, R. G.; Sundstroem, V. & Polivka, T. (2002). Carotenoid to chlorophyll energy transfer in the peridinin-chlorophyll a-protein complex involves an intramolecular charge transfer state. *Proceedings of the National Academy of Sciences of the United States of America*. 99, 26, (December 2002), pp. 16760-16765 ISSN 0027-8424
- Zigmantas, D.; Hiller, R. G.; Sharples, F. P.; Frank, H. A.; Sundstrom, V. & Polivka, T. Effect of a conjugated carbonyl group on the photophysical properties of carotenoids. *Physical Chemistry Chemical Physics*. 6, 11, (June 2004), pp. 3009-3016 ISSN 1463-9076
- Vaswani, H. M.; Hsu, C. P.; Head-Gordon, M. & Fleming, G. R. Quantum chemical evidence for an intramolecular charge-transfer state in the carotenoid peridinin of peridinin-chlorophyll-protein. *Journal of Physical Chemistry B*. 107, 31, (August 2003), pp. 7940-7946 ISSN 1520-6106

IntechOpen



### **Artificial Photosynthesis**

Edited by Dr Mohammad Najafpour

ISBN 978-953-307-966-0

Hard cover, 288 pages

**Publisher** InTech

**Published online** 24, February, 2012

**Published in print edition** February, 2012

Photosynthesis is one of the most important reactions on Earth, and it is a scientific field that is intrinsically interdisciplinary, with many research groups examining it. We could learn many strategies from photosynthesis and can apply these strategies in artificial photosynthesis. Artificial photosynthesis is a research field that attempts to replicate the natural process of photosynthesis. The goal of artificial photosynthesis is to use the energy of the sun to make different useful material or high-energy chemicals for energy production. This book is aimed at providing fundamental and applied aspects of artificial photosynthesis. In each section, important topics in the subject are discussed and reviewed by experts.

#### **How to reference**

In order to correctly reference this scholarly work, feel free to copy and paste the following:

Takayuki Kajikawa and Shigeo Katsumura (2012). An Approach Based on Synthetic Organic Chemistry Toward Elucidation of Highly Efficient Energy Transfer Ability of Peridinin in Photosynthesis, *Artificial Photosynthesis*, Dr Mohammad Najafpour (Ed.), ISBN: 978-953-307-966-0, InTech, Available from: <http://www.intechopen.com/books/artificial-photosynthesis/a-new-approach-based-on-a-synthetic-organic-chemistry-toward-elucidation-of-highly-efficient-energy->

**INTECH**  
open science | open minds

#### **InTech Europe**

University Campus STeP Ri  
Slavka Krautzeka 83/A  
51000 Rijeka, Croatia  
Phone: +385 (51) 770 447  
Fax: +385 (51) 686 166  
[www.intechopen.com](http://www.intechopen.com)

#### **InTech China**

Unit 405, Office Block, Hotel Equatorial Shanghai  
No.65, Yan An Road (West), Shanghai, 200040, China  
中国上海市延安西路65号上海国际贵都大饭店办公楼405单元  
Phone: +86-21-62489820  
Fax: +86-21-62489821

© 2012 The Author(s). Licensee IntechOpen. This is an open access article distributed under the terms of the [Creative Commons Attribution 3.0 License](#), which permits unrestricted use, distribution, and reproduction in any medium, provided the original work is properly cited.

IntechOpen

IntechOpen